

# Electronic structure and transport for a laser-field-irradiated quantum wire with Rashba spin-orbit coupling

Guanghai Zhou<sup>1,2,3\*</sup> and Wenhui Liao<sup>2</sup>

<sup>1</sup>*CCAST (World Laboratory), PO Box 8730, Beijing 100080, China*

<sup>2</sup>*Department of Physics, Hunan Normal University, Changsha 410081, China<sup>†</sup> and*

<sup>3</sup>*International Center for Materials Physics, Chinese Academy of Sciences, Shenyang 110015, China*

We investigate theoretically the electronic structure and transport for a two-level quantum wire with Rashba spin-orbit coupling (SOC) under the irradiation of an external laser field at low temperatures. The photon-induced transitions between SOC-split subbands with the same lateral confinement quantum numbers and between subbands with different confinement quantum number are expected. Using the method of equation of motion (EOM) for Keldysh nonequilibrium Green's functions (NGF), we examine the time-averaged density of states (DOS) and the spin polarized conductance for the system with photon polarization perpendicular to the wire direction. Through the analytical analysis and some numerical examples, the interplay effects of the external laser field and the Rashba SOC on both the DOS and the conductance of the system are demonstrated and discussed. It is found that the external laser field can adjust the spin polarization rate and the transport of the quantum wire system with some proper Rashba SOC strengths.

PACS numbers: 73.23.-b, 71.70.Ej, 72.25.-b, 78.67.Lt

## I. INTRODUCTION

In recent years, the effects of SOC in semiconductor mesoscopic systems have attracted more and more attention since it plays an important role in the emerging field of spintronics (see recent review article<sup>1</sup> and references therein) since the proposal of constructing an electronic analog of optic modulator using ferromagnetic contacts as the spin injector and the detector.<sup>2</sup> Many fundamental and interesting phenomena, such as spin precession,<sup>3,4</sup> spin accumulation,<sup>5,6</sup> spin (polarized) transport<sup>7,8</sup> and spin Hall effect<sup>9,10</sup> in the systems with SOC have been investigated and are under further study now. Though the SOC has its origin in relativistic effects, it is regarded vitally in some low-dimensional mesoscopic semiconductor systems.<sup>11,12</sup>

Usually, two types of SOC are taken into account in the investigation for systems based on a two-dimensional electron gas (2DEG) confined in a semiconductor heterostructure. They are Rashba<sup>11</sup> and Dresselhaus<sup>12</sup> SOC, which can be described by the Hamiltonians

$$H_R = \frac{\hbar k_R}{m^*} (\sigma_x p_y - \sigma_y p_x) \quad (1)$$

and

$$H_D = \frac{\hbar k_D}{m^*} (\sigma_y p_y - \sigma_x p_x), \quad (2)$$

respectively, where  $m^*$  is the effective electron mass and  $\sigma = (\sigma_x, \sigma_y, \sigma_z)$  is the vector of Pauli matrix. The strengths of the two types of SOC are measured in terms of characteristic wavevectors  $k_R$  and  $k_D$ , respectively. For some semiconductor based systems (e.g.,

InAs quantum well), the Rashba term arising from the structure inversion asymmetry in heterostructures<sup>13,14</sup> is roughly one order magnitude larger than Dresselhaus term which is due to the bulk inversion asymmetry.<sup>15</sup> Moreover, the strength of Rashba SOC can be tuned by external gate voltage,<sup>16</sup> and its effect on the systems has been paid more attention, particularly in quasi-one-dimensional quantum wire system.

Mesoscopic systems with or without external magnetic field in the presence of SOC have been studied extensively.<sup>3-10,17</sup> Two years ago, two independent experiments on the (001)-grown n-type GaAs multiple quantum well structures had been done by using a circularly polarized infrared radiation<sup>18</sup> and the orthogonally polarized two optical harmonic pulses,<sup>19</sup> respectively. The spin photocurrent<sup>18</sup> and the pure spin current<sup>19</sup> due to resonant intersubband transitions have been observed in the absence of any external magnetic field. Hereafter, for a single quantum well (2DEG) with SOC irradiated under an in-plane linearly polarized infrared irradiation, the spin-dependent density of state (DOS) and the density of spin polarization has been calculated, and a pure spin current has been theoretically verified for the system.<sup>20</sup> Further, a mechanism for spin-polarized photocurrent generation in a multimode quantum wire, which is due to the combined effect of the Rashba SOC and a linearly polarized in-plane microwave irradiation, has been proposed in the presence of a static in-plane magnetic field.<sup>21</sup> On the other hand, the electron transport for a quantum wire under a time-varying electromagnetic (EM) field irradiation in the absence of SOC has been analyzed previously by means of the NGF<sup>22</sup> and the scattering matrix approach,<sup>23</sup> respectively. However, a further confined low-dimensional systems, such as a two-level quasi-one-dimensional quantum wire or quasi-zero-dimensional quantum dot with SOC under the irradiation of time-dependent field have

<sup>†</sup>Mailing address

been studied rarely.<sup>21</sup>

Mesoscopic two-level system (such as a two-level quantum wire or quantum dot) is of physically important since it has been proved to be very useful in describing many aspects of interaction between EM field and the electrons confined in a heterostructure, and in application of solid-state electronic device. Therefore, it is meaningful to investigate the interplay effect between the SOC and the applied laser field for a two-level mesoscopic system.

In order to investigate the electronic structure and transport of a two-level quantum wire with SOC under an intense laser field irradiation, in this paper we theoretically calculate the time-averaged DOS and the conductance at the low temperatures for the system. The interplay effects of different laser frequency and Rashba SOC strength on the electronic structure and transport are investigated by using the nonequilibrium Keldysh formalism (NKF). Through the analysis with a few numerical examples, we find some characteristics different from those for the similar systems in previous works.<sup>20–23</sup>

The remainder part of the paper is organized as follows. In Sec. II, we introduce the model Hamiltonian for our system and give the NKF straightforwardly, where the time-averaged DOS and the conductance are calculated analytically. The numerical results and the discussions are shown in Sec. III. Finally, Sec. IV concludes the paper.

## II. MODEL AND FORMALISM

The NGF approach has been employed in last decades to study a variety of problems beyond the linear response regime.<sup>22</sup> Meir et al<sup>24</sup> derived a formula for the current through a region of interacting electrons using the NKF. Changing the one-direction time axis into a loop with two branches, four Green's functions depending on the relative positions of  $t_a$  and  $t_b$  in the loop can be defined. They are time-ordered, anti-time-ordered and two distribution Green's functions, respectively. However, only two of them are independent. We will use the approach of standard nonequilibrium Keldysh EOM in the present work.

Consider a quasi-one-dimensional system of electrons (a quantum wire) in the presence of SOC and an external time-dependent laser field, the model Hamiltonian reads

$$H = \frac{\mathbf{p}^2}{2m^*} + V(\mathbf{r}) + H_{so} + V(t), \quad (3)$$

where  $\mathbf{r} = (x, y)$  and  $\mathbf{p} = (p_x, p_y)$  are two-dimensional position and momentum vectors, respectively. The SOC Hamiltonian  $H_{so}$  is generally consisted of  $H_R$  and  $H_D$ , while  $V(t)$  is the potential from the interaction of the external time-dependent laser field with electrons in the system. The electrons are confined in the  $y$  direction by

an infinite square-well potential of width  $a$ , i.e.,

$$V(\mathbf{r}) = \begin{cases} 0 & (|y| < a/2) \\ \infty & (|y| > a/2), \end{cases} \quad (4)$$

which can eliminate the possibility of SOC due to the effective electric field coming from the nonuniformity of the confining potential.<sup>25</sup>

To investigate the effects of SOC and the external field on the electron transport properties by means of NKF, we rewrite Hamiltonian (3) in the second-quantized form. For this purpose, we define that  $a_{ks\alpha}^+$  ( $a_{ks\alpha}$ ) creates (annihilates) an electron with wavevector  $k$  and a spin branch  $s$  [ $s = \uparrow$  and  $\downarrow$ , or  $+$  and  $-$ , which is the spin branch index corresponding to spin-up and spin-down, respectively. See Eq.(11) for detailed explanation] in mode  $\alpha$  in either the left (L) or the right (R) lead, and  $c_{k_x n s}^+$  ( $c_{k_x n s}$ ) creates (annihilates) an electron in the  $n$ th transverse mode  $|k_x, n, s\rangle$  with wavevector  $k_x$  and a spin branch index  $s$  in the absence of SOC in the quantum wire modeled as a two-level ( $n = 1, 2$ ) system. For convenience, we choose<sup>25</sup> the spin polarization axis  $\hat{\mathbf{n}} = (\cos\varphi, \sin\varphi)$  to be along the effective magnetic field due to the SOC for wave propagating in the  $x$ -direction such that

$$|s\rangle = \frac{1}{\sqrt{2}} \begin{pmatrix} se^{-i\varphi/2} \\ e^{i\varphi/2} \end{pmatrix} \quad (5)$$

with  $\varphi \equiv \arg[k_D + ik_R]$ . With these definitive operators and spin states, the Hamiltonian for a laser-field-irradiated two-level quantum wire (connected to two electrode leads) in the presence of SOC reads

$$\begin{aligned} H = & \sum_{k,s,\alpha \in L/R} \varepsilon_{ks\alpha} a_{ks\alpha}^+ a_{ks\alpha} + \sum_{k_x, n, s} \varepsilon_{ns}(k_x) c_{k_x n s}^+ c_{k_x n s} \\ & + \sum_{k, k_x, n, s, \alpha \in L/R} (T_{kk_x n s}^\alpha a_{ks\alpha}^+ c_{k_x n s} + h.c.) \\ & + \sum_{k_x, n, n', s, s'} [\gamma_{nn'} \beta_{ss'} + V_{nsn's'} \cos(\Omega t)] c_{k_x n s}^+ c_{k_x n' s'} \end{aligned} \quad (6)$$

where  $\varepsilon_{ks\alpha}$  is the energy level with spin  $s$  and wavevector  $k$  in lead  $\alpha$ , and

$$\varepsilon_{ns}(k_x) = \frac{\hbar^2}{2m^*} [(k_x - sk_{so})^2 + (\frac{n\pi}{a})^2] - \Delta_{so} \quad (7)$$

is the  $n$ th sublevel in the wire with  $k_{so} = \sqrt{k_R^2 + k_D^2}$  and  $\Delta_{so} = \hbar^2 k_{so}^2 / 2m$ . In Hamiltonian (6), the coupling between the electrode leads and the wire with strength  $T_{kk_x n s}^\alpha$  is represented by the third term, and the last term describes the adiabatical electron-photon interaction in the wire<sup>22,26</sup> and the mixture of transverse modes due to SOC, where  $V_{nsn's'}$  are the dipole electron-photon interaction matrix elements (MEs) and  $\Omega$  the incident laser frequency. Since the frequencies of interest are in the range corresponding to wavelengths of the order of hundreds of nanometers, the spatial variation of the field potential can be neglected. The SOC mixes the transverse

modes through the matrix element  $\gamma_{nn'}\beta_{ss'}$ , where

$$\gamma_{nn'} = \frac{4nn'}{a(n^2 - n'^2)} \begin{cases} (-1)^{\frac{n+n'-1}{2}} & (n \neq n') \\ 0 & (n = n') \end{cases}, \quad (8)$$

and according to the lateral confinement potential<sup>25</sup>  $\beta_{ss'}$  is the element of matrix

$$\beta = \frac{\hbar^2}{m^*k_{so}} \begin{bmatrix} 2ik_Rk_D & k_D^2 - k_R^2 \\ k_R^2 - k_D^2 & -2ik_Rk_D \end{bmatrix}. \quad (9)$$

In the above Hamiltonian we have neglected electron-electron interactions since its effect on SOC can be plausibly taken into a renormalized SOC constant.<sup>27</sup>

For simplicity, we focus on the Rashba SOC effect, i.e., let  $k_D = 0$ . Furthermore, according to Dyson equation, the coupling between the electrode leads and the wire only adds a self-energy term in the NGF, so we firstly calculate the Green's function (GF) of the quantum wire without considering the electrode leads. In this case the Hamiltonian of the quantum wire part in the absence of EM field reads

$$\begin{aligned} H_{wire} = & \sum_{k_x} [\varepsilon_{1\uparrow}(k_x)c_{k_x,1\uparrow}^+c_{k_x,1\uparrow} + \varepsilon_{1\downarrow}(k_x)c_{k_x,1\downarrow}^+c_{k_x,1\downarrow} \\ & + \varepsilon_{2\uparrow}(k_x)c_{k_x,2\uparrow}^+c_{k_x,2\uparrow} + \varepsilon_{2\downarrow}(k_x)c_{k_x,2\downarrow}^+c_{k_x,2\downarrow} \\ & + \varepsilon_R(c_{k_x,2\uparrow}^+c_{k_x,1\downarrow} + c_{k_x,1\downarrow}^+c_{k_x,2\uparrow} \\ & - c_{k_x,1\uparrow}^+c_{k_x,2\downarrow} - c_{k_x,2\downarrow}^+c_{k_x,1\uparrow})], \end{aligned} \quad (10)$$

where  $\varepsilon_R = 8\hbar^2k_R/(3m^*a)$ . According to Eq.(5), here the spin-up state  $|\uparrow\rangle$  and the spin-down state  $|\downarrow\rangle$  are the linear combination of the eigenstates of  $\sigma_z$

$$\begin{aligned} |\uparrow\rangle &= \frac{1-i}{2} \begin{pmatrix} 1 \\ 0 \end{pmatrix} + \frac{1+i}{2} \begin{pmatrix} 0 \\ 1 \end{pmatrix}, \\ |\downarrow\rangle &= -\frac{1-i}{2} \begin{pmatrix} 1 \\ 0 \end{pmatrix} + \frac{1+i}{2} \begin{pmatrix} 0 \\ 1 \end{pmatrix}, \end{aligned} \quad (11)$$

with equal probability occupying the real spin-up and spin-down states in the original spin space, respectively.

For definiteness, we consider the case of the applied incident laser is polarized along  $y$  direction (perpendicular to the wire direction), hence the diagonal electron-photon interaction MEs are simply zero in the dipole approximation. Also for simplicity in calculation we assume phenomenologically that the off-diagonal electron-photon interaction MEs  $V_{1s2s'} = V_{2s1s'} = 1.0$  as the free input parameters (dependent of incident laser intensity), and thus the Hamiltonian (10) becomes

$$\begin{aligned} H'_{wire} = & \sum_{k_x} \{ \varepsilon_{1\uparrow}(k_x)c_{k_x,1\uparrow}^+c_{k_x,1\uparrow} + \varepsilon_{1\downarrow}(k_x)c_{k_x,1\downarrow}^+c_{k_x,1\downarrow} \\ & + \varepsilon_{2\uparrow}(k_x)c_{k_x,2\uparrow}^+c_{k_x,2\uparrow} + \varepsilon_{2\downarrow}(k_x)c_{k_x,2\downarrow}^+c_{k_x,2\downarrow} \\ & + \frac{1}{2}(e^{i\Omega t} + e^{-i\Omega t}) + \varepsilon_R)(c_{k_x,1\downarrow}^+c_{k_x,2\uparrow} + c_{k_x,2\uparrow}^+c_{k_x,1\downarrow}) \\ & + \frac{1}{2}(e^{i\Omega t} + e^{-i\Omega t}) - \varepsilon_R)(c_{k_x,1\uparrow}^+c_{k_x,2\downarrow} + c_{k_x,2\downarrow}^+c_{k_x,1\uparrow}) \\ & + \frac{1}{2}(e^{i\Omega t} + e^{-i\Omega t})(c_{k_x,1\uparrow}^+c_{k_x,2\uparrow} + c_{k_x,2\uparrow}^+c_{k_x,1\uparrow} \\ & + c_{k_x,1\downarrow}^+c_{k_x,2\downarrow} + c_{k_x,2\downarrow}^+c_{k_x,1\downarrow}) \}. \end{aligned} \quad (12)$$

It is seen from Eqs.(10) and (12) that the pure Rashba SOC induces spin-flip transitions with equal probabilities (spin-conserving) according to Eq.(6) while the applied laser field may arouse unequal probability transitions for spin-flip and spin-conserving due to the interplay between the Rashba SOC and the field. Our interest is to numerically find which kind of transitions is favorable for this system.

Next we employ the usually defined retarded GF<sup>22,24</sup>

$$\begin{aligned} G_{n's'n'}^r(t_2, t_1) &= \ll c_{k_x n s}(t_2), c_{k_x n' s'}(t_1) \gg^r \\ &= -i\theta(t_2 - t_1) \langle \{ c_{k_x n s}(t_2), c_{k_x n' s'}(t_1) \} \rangle, \end{aligned} \quad (13)$$

then its corresponding Keldysh EOM is

$$\begin{aligned} i\frac{\partial}{\partial t_2} \ll c_{k_x n s}(t_2), c_{k_x n' s'}(t_1) \gg^r &= \\ \delta(t_2 - t_1) \langle \{ c_{k_x n s}(t_2), c_{k_x n' s'}(t_1) \} \rangle & \\ + \ll [c_{k_x n s}(t_2), H], c_{k_x n' s'}(t_1) \gg^r. & \end{aligned} \quad (14)$$

Inserting system Hamiltonian (12) into (14) and transforming the variables to  $t_2 - t_1$  and  $t_1$ , and then performing the Fourier transform to change the variable  $t_2 - t_1$  into  $\omega$ , we finally obtain the diagonal MEs of the two retarded GFs without the coupling between the electrode leads and the wire

$$\begin{aligned} \{ [\omega - \varepsilon_{1/2\uparrow}(k_x)][\omega - \varepsilon_{2/1\downarrow}(k_x)] - \varepsilon_R^2 \} \\ \cdot \ll c_{k_x,1/2\uparrow}, c_{k_x,1/2\uparrow}^+ \gg_\omega^r = \omega - \varepsilon_{2/1\downarrow}(k_x), \end{aligned} \quad (15)$$

$$\begin{aligned} \{ [\omega - \varepsilon_{1/2\downarrow}(k_x)][\omega - \varepsilon_{2/1\uparrow}(k_x)] - \varepsilon_R^2 \} \\ \cdot \ll c_{k_x,1/2\downarrow}, c_{k_x,1/2\downarrow}^+ \gg_\omega^r = \omega - \varepsilon_{2/1\uparrow}(k_x), \end{aligned} \quad (16)$$

$$\begin{aligned} [\omega - \varepsilon_{1/2\uparrow}(k_x)] \ll c_{k_x,1/2\uparrow}, c_{k_x,1/2\uparrow}^+(t_1) \gg_\omega^r \\ = 1 \mp \varepsilon_R \ll c_{k_x,2/1\downarrow}, c_{k_x,1/2\uparrow}^+(t_1) \gg_\omega^r \\ + \frac{1}{2}e^{i\Omega t_1} [\ll c_{k_x,2/1\downarrow}, c_{k_x,1/2\uparrow}^+(t_1) \gg_{\omega+\Omega}^r \\ + \ll c_{k_x,2/1\uparrow}, c_{k_x,1/2\uparrow}^+(t_1) \gg_{\omega+\Omega}^r] \\ + \frac{1}{2}e^{-i\Omega t_1} [\ll c_{k_x,2/1\downarrow}, c_{k_x,1/2\uparrow}^+(t_1) \gg_{\omega-\Omega}^r \\ + \ll c_{k_x,2/1\uparrow}, c_{k_x,1/2\uparrow}^+(t_1) \gg_{\omega-\Omega}^r], \end{aligned} \quad (17)$$

$$\begin{aligned} [\omega - \varepsilon_{1/2\downarrow}(k_x)] \ll c_{k_x,1/2\downarrow}, c_{k_x,1/2\downarrow}^+(t_1) \gg_\omega^r \\ = 1 \pm \varepsilon_R \ll c_{k_x,2/1\uparrow}, c_{k_x,1/2\downarrow}^+(t_1) \gg_\omega^r \\ + \frac{1}{2}e^{i\Omega t_1} [\ll c_{k_x,2/1\uparrow}, c_{k_x,1/2\downarrow}^+(t_1) \gg_{\omega+\Omega}^r \\ + \ll c_{k_x,2/1\downarrow}, c_{k_x,1/2\downarrow}^+(t_1) \gg_{\omega+\Omega}^r] \\ + \frac{1}{2}e^{-i\Omega t_1} [\ll c_{k_x,2/1\uparrow}, c_{k_x,1/2\downarrow}^+(t_1) \gg_{\omega-\Omega}^r \\ + \ll c_{k_x,2/1\downarrow}, c_{k_x,1/2\downarrow}^+(t_1) \gg_{\omega-\Omega}^r], \end{aligned} \quad (18)$$

for spin-up and spin-down, respectively. It is seen from Eqs.(17) and (18) that the retard NGF  $G_0^r$  with frequency

$\omega$  are coupled to the components with photon sideband frequencies of  $\omega + \Omega$  and  $\omega - \Omega$  in connection with  $k_{so}$  (the characteristic wavevector of Rashba SOC).

On the other hand, the self-energy describing the influence of the leads on the system can be simply written as

$$\Sigma_{nn'} \equiv \Sigma_{nn'}^{L/R}(\omega) = 2\pi \sum_{k,k_x,s} (T_{kk_xns}^\alpha)^* T_{k,k_xn's}^\alpha \delta(\omega - \varepsilon_{ks\alpha}), \quad (19)$$

with which one can construct the GF  $G^r = [(G_0^r)^{-1} - i\Sigma]^{-1}$  for the whole system. If we calculate the time-averaged NGF up to the second order, then at low temperatures the time-averaged DOS is

$$DOS = -\frac{1}{\pi} \text{Im}[Tr(G^r(\omega, \omega))], \quad (20)$$

and the conductance has the form of Landauer-type<sup>22,26</sup>

$$G = \frac{e^2}{h} Tr[\Sigma^L(\omega) G^a(\omega, \omega) \Sigma^R(\omega) G^r(\omega, \omega)]. \quad (21)$$

Here  $G^r(\omega, \omega)$  and  $G^a(\omega, \omega)$  represent the time-averaged retarded and advanced GFs, respectively.

### III. NUMERICAL RESULTS AND DISCUSSIONS

In the following, we present some numerical examples of the DOS and conductance calculated according to Eqs. (15)-(21) for the system. We have selected that the energy unit  $E^* = \epsilon_1 = \pi^2 \hbar^2 / (2m^* a^2)$  (i.e., the first lateral level of the quantum wire without SOC), the time unit  $t^* = \hbar / E^*$ , and the frequency unit  $\Omega^* = 1/t^*$ . With these units, the propagating longitudinal wavevector corresponding to the  $n$ th transverse mode is  $k_x = (\omega - n^2)^{1/2}$ . In the wide-band approximation the real part of the self-energy is negligible,<sup>22,24-26</sup> and we simply assume that  $\Sigma_{11} = \Sigma_{22} = 0.1$  and  $\Sigma_{12} = \Sigma_{21} = 0.05$ . The choice of these typical parameters is based on the following consideration.<sup>22</sup> Usually the strength of electron-photon interaction depends on the photon intensity, polarization and the size of the quantum wire. Under the irradiation of a strong laser with an electric field of the order  $(10^5 - 10^6)$  V/m, the MEs are comparable to or several times larger than the level spacing in the quantum wire with the width of order  $(10 - 100)$  nm (corresponding to the external laser frequency  $\sim$  THz), and these quantities are physically realizable in recent experiments.<sup>18,19</sup>

We first consider the electronic structure of the system. It is common known that the electronic energy spectrum is degenerate for the two spin orientation in the absence of SOC. In the presence of SOC the energy spectrum (7) satisfies the condition  $\varepsilon_{n,s}(k_x) = \varepsilon_{n,-s}(-k_x)$  in accordance with the time inversion symmetry. However, our interest is the interplay effect of the external laser field and the Rashba SOC on the electronic structure

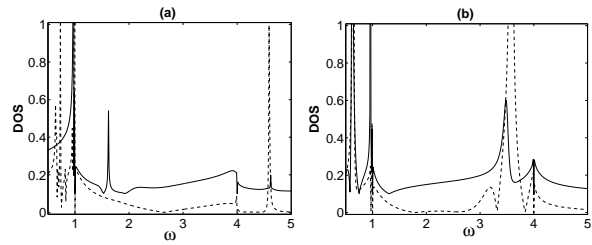


FIG. 1: The time-averaged DOS (in arbitrary units) as a function of energy with electron-photon interaction off-diagonal matrix elements  $V_{1s2s'} = V_{2s1s'} = 1.0$  for the two different Rashba SOC strengths (a)  $k_R = 1/(2\pi)$  and (b)  $k_R = 1/\pi$ , where the incident laser frequency is  $\Omega = 0.5$  and the solid (dashed) line represents the spin-up (-down) is shifted 0.1 upward for clarity.

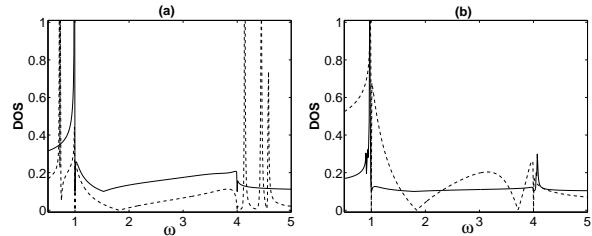


FIG. 2: The time-averaged DOS (in arbitrary units) as a function of energy with the same system parameters and line presentation as in Fig.2 except for the incident laser energy is  $\Omega = 3.0$ .

and transport of the system. Here we consider that the incident field is linearly polarized perpendicular to the current direction (the wire direction), i.e., the off diagonal MEs dominate the electron-photon interaction. With the assumption of the off diagonal MEs  $V_{12} = V_{21} = 1.0$  [see Eq.(11)] and the incident laser frequency  $\Omega = 0.5$ , in Fig.1 we illustrate the time-averaged DOS as a function of energy for the two different Rashba SOC strengths  $k_R = 1/(2\pi)$  and  $k_R = 1/\pi$ , respectively. We can see that the main peak around  $\omega \sim 1$  is always obvious in the presence of both Rashba SOC and laser field. This is because that the electrons are populated at energy level  $\varepsilon_{1\uparrow} \sim 1.01$  rather than  $\varepsilon_{1\downarrow} \sim 1.25$  with single photon absorption. In the case of weak Rashba SOC strength as shown in Fig.1(a), there are two additional photon resonance peaks at  $\omega = 1.6$  and  $4.6$  for spin-up (solid line), while for spin-down (dashed line) there are three additional resonance peaks at  $\omega = 4.58, 0.75$  and  $0.65$  with a pattern of oscillation in the range of  $0.76 < \omega < 1$ . Nevertheless, as the increase of the Rashba SOC strength shown in Fig.1(b), for spin-up the two photon resonance peaks are shifted from  $\omega = 1$  and  $4$  to  $\omega = 0.63$  and  $3.4$ , respectively. While for spin-down there only two resonance peaks occur at  $\omega = 0.63$  (superposed with that for spin-up) and  $3.5$  without an oscillatory pattern. However, it seems that the other main peak around  $\omega \sim 4$  makes sense in this strong Rashba SOC case. Because the single photon

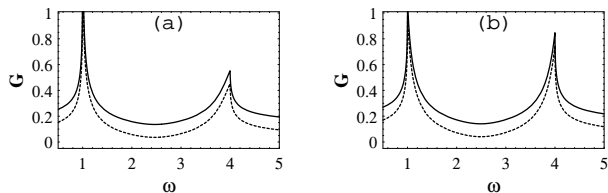


FIG. 3: The plotted conductance  $G$  (in the unit of  $e^2/h$ ) as a function of energy ( $\sim \omega$ , in unit of  $\epsilon_1$ ) without laser field for the two different Rashba SOC strengths (a)  $k_R = 1/(2\pi)$  and (b)  $k_R = 1/\pi$ , where the solid (dashed) line represents the spin-up (-down) is shifted 0.1 upward for clarity.

energy  $\Omega$  is much smaller than the quantum wire sublevel spacing  $\Delta\epsilon$ , the resonance peaks here are belong to the transitions between Rashba SOC-splitted subbands with the same lateral confinement quantum number.<sup>21</sup>

In order to determine the transitions between subbands with different confinement quantum number, in Fig.2 we increase the incident frequency to  $\Omega = 3$  but with the same two different Rashba SOC strengths as in Fig.1. As shown in Fig.2 the time-averaged DOS for spin-up (solid lines) has no transition resonance peaks in the both weak and strong Rashba SOC cases, while for spin-down there are several sharp resonance transition peaks at  $\omega=0.75, 4.1, 4.5$  and  $4.6$  in the weak Rashba SOC case [see the dashed line in Fig.2(a)] and an oscillatory pattern with no resonance peak [dashed line in Fig.2(b)] in the strong Rashba SOC case. This result implies a rule of possible transition that the transition probabilities are very larger for this condition. We believe that some of the resonance peaks in Fig.2(a) can be identified to the photon-induced transitions between subbands with different quantum numbers.<sup>21-23</sup> Because both spin-flip and spin-conserving transitions are modulated by the strengths of Rashba SOC and laser field, so it seems that the strong strength of Rashba SOC in the higher laser frequency case is not favorable for the transitions between subbands with different quantum numbers.

Next we turn our attention to the conductance of the system. The conductance (in unit of  $e^2/h$ ) as a function of energy ( $\sim \omega$ , in unit of  $\epsilon_1$ ) of the system without external laser field in the presence of weak and strong Rashba SOC is illustrated in Fig.3. There are two major peaks in the conductance curves, as a consequence of the two subband levels structure of the wire. Particularly, the conductance difference for the two spin orientation in Fig.3 is very small and consistent with the analytical prediction from energy spectrum. One also note that the conductance peaks are asymmetry near the two subband levels due to the spin-orbit interaction.<sup>26</sup>

The time-averaged conductance of the system irradiated under a transversally polarized laser field in the presence of Rashba SOC is shown in Fig.4 with  $\Omega = 0.5$ . Corresponding to the resonance states in Fig.1(a), the time-averaged conductance in Fig.4(a) shows some peaks with the height of  $\sim e^2/h$ . When the incident electrons

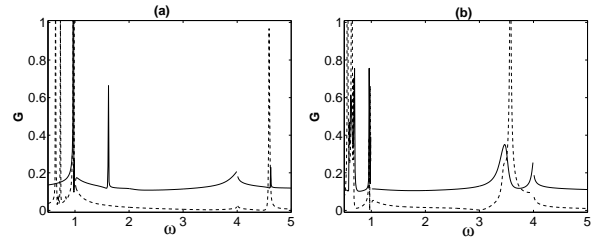


FIG. 4: The time-averaged conductance  $G$  (in the unit of  $e^2/h$ ) as a function of energy with the same system parameters and line presentation as in Fig.1.

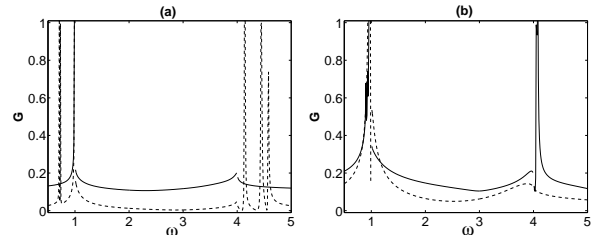


FIG. 5: The time-averaged conductance  $G$  (in the unit of  $e^2/h$ ) as a function of energy with the same system parameters and line presentation as in Fig.2.

energy is about  $\omega = 0.65$  and  $0.75$ , we note that the conductance is nearly  $e^2/h$  for spin-down while that for spin-up is nearly 0; when the incident electrons energy is increased to  $\omega = 1.6$ , there is a sharp conductance peak for spin-up while that for spin-down is about 0. Therefore, with a largest spin polarization in Fig.1(a), a spin filter may be devised in the case of appropriate incident electron energy and the Rashba SOC strength. Fig.4(b) shows the time-averaged conductance corresponding to the Fig.1(b) in strong Rashba SOC case, from which one can see more photon resonance peaks (especially in lower energy range) than in the weak Rashba SOC case. Furthermore, when the external laser frequency is increased to 3.0 the time-averaged conductance of the system with the two different Rashba SOC strengths is illustrated in Fig.5. Due to the intersubband resonance states in Fig.2(a), there is more sharp resonance transition peaks in higher energy range [see Fig.5(a)] for the spin-down electrons [see the explanation for Fig.2(a)]. While in the strong Rashba SOC case, the conductance curves for both spin-up and -down show only the two main peaks [see Fig.5(b)] as in Fig.2(b). Maybe in this case the Rashba SOC is too strong to produce quantum transitions for the system.

Finally, the time-averaged DOS (solid line for spin-up and dash-dotted line for spin-down) and the spin polarization rate<sup>20</sup> (dashed line) with a fixed incident electron energy ( $\omega = 2.5$ ) as a function of the characteristic wavevector  $k_R$  (proportional to the strength of Rashba SOC) without or with a transversally polarized external laser field ( $\Omega = 0.5$ ) are demonstrated in Fig.6(a) and Fig.6(b), respectively. The electronic energy spectrum

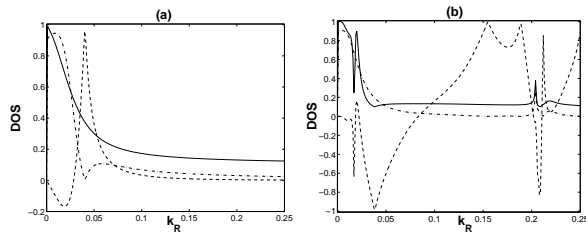


FIG. 6: The time-averaged DOS and spin polarization rate as a function of  $k_R$  (proportional to the strength of Rashba SOC) for a fixed incident electrons energy  $\omega = 2.5$  (a) without and (b) with a transversally polarized laser field ( $\Omega = 0.5$ ), where the solid line (shifted 0.1 upward for clarity) for spin-up and dash-dotted line for spin-down DOS, respectively. The dashed line represents spin polarization rate.

is degenerate for spin-up and spin-down when  $k_R = 0$  in both cases as expected (see the solid and dash-dotted lines in Fig.6). In the case without laser field as shown in Fig.6(a), the spin polarization rate (dashed line) is about 17% when  $k_R = 0.02$ , and it can reach to 95% when  $k_R = 0.04$ . Under the irradiation of the laser field, as shown in Fig.6(b), the spin polarization rate increases to 60% and 100% around  $k_R = 0.02$  and  $k_R = 0.04$ , respectively. Moreover, there are several additional peaks of spin polarization rate in the range of  $0.05 < k_R < 0.25$  with laser field, while in the case without laser field as shown in Fig.6(a) the spin polarization rate is smoothly low in this range of  $k_R$ . Therefore, it seems that the external laser field can enhance the spin polarization rate for a quantum wire system with an appropriate Rashba

SOC strength which can be adjusted through the controllable lateral electrodes.<sup>16</sup>

#### IV. CONCLUSION

In summary, using the method of EOM for Keldysh NGF, we have investigated theoretically the electronic structure and transport properties of a two-sublevel quantum wire irradiated under a transversally polarized external laser field in the presence of Rashba SOC. The time-averaged DOS and conductance for spin-up and spin-down electrons in the case of the off-diagonal electron-photon interaction dominating the process are calculated analytically, and are demonstrated numerically with two different Rashba SOC strengths and laser frequencies, respectively. It is found that the external laser field can enhance the spin polarization rate for the system with some particular Rashba SOC strengths. An all-electrical nonmagnetic spintronic devices may be desirable under an appropriate choice of external control parameters. However, the experimental observation for this proposal and further theoretical investigation if the impurity, phonon or electron-electron interaction are taken into account are worthy to be carried out.

#### Acknowledgments

This work was supported by National Natural Science Foundation of China (Grant NO. 10574042), and by Scientific Research Fund of Hunan Provincial Education Department (Grant NO. 04A031).

- 
- \* Electronic address: ghzhou@hunnu.edu.cn
- 1 Zutic I, Fabian J and Sarma S D 2004 Rev. Mod. Phys. **76** 323
  - 2 Datta S and Das B 1990 Appl. Phys. Lett. **56** 665
  - 3 Mireles F and Kirczenow G 2004 Phys. Rev. B **64** 024426  
Winkler R 2004 Phys. Rev. B **69** 045317
  - 4 Liu Ming-Hao, Chang Ching-Ray and Chen Son-Hsien 2005 Phys. Rev. B **71** 153305
  - 5 Governale M and Zülicke U 2002 Phys. Rev. B **66** 073311
  - 6 Onoda M and Nagaosa N 2005 Phys. Rev. Lett. **95** 106601  
Onoda M and Nagaosa N 2005 Phys. Rev. B **72** 081301(R)
  - 7 Balents L and Egger R 2000 Phys. Rev. Lett. **85** 3464  
Pramanik S, Bandyopadhyay S and Cahay M 2003 Phys. Rev. B **68** 075313
  - 8 Rodrigues V, Bettini J, Silva P C and Ugarte D 2003 Phys. Rev. Lett. **91** 096801  
Wang X F, Vasilopoulos P and Peeters F M 2005 Phys. Rev. B **71** 125301
  - 9 Murakami S, Nagaosa N and Zhang S C 2003 Science **301** 1348  
Murakami S, Nagaosa N and Zhang S C 2004 Phys. Rev. B **69** 235206
  - 10 Hirsch J E 1999 Phys. Rev. Lett. **83** 1834 (1999)  
Sinova J, Culcer D, Niu Q, Sinitsyn N A, Jungwirth T and MacDonald A H 2004 Phys. Rev. Lett. **92** 126603
  - Shen Shun-Qing, Michael Ma, Xie X C and Fu Chun Zhang 2004 Phys. Rev. Lett. **92** 256603
  - 11 Bychkov Y A and Rashba E I 1984 J. Phys. C **17** 6039
  - 12 Dresselhaus G 1955 Phys. Rev. B **100** 580
  - 13 Lommer G, Malcher F and Rössler U 1988 Phys. Rev. Lett. **60** 728
  - 14 Andradæ Silva E A, Rocca G C L and Bassani F 1994 Phys. Rev. B **50** 8523
  - 15 Moroz A V and Barnes C H W 1999 Phys. Rev. B **60** 14272
  - 16 Nitta J, Akazaki T, Takayanagi H and Enoki T 2002 Phys. Rev. Lett. **78** 1335  
Grundler D 2000 Phys. Rev. Lett. **84** 6074  
Koga T, Nitta J, Akazaki T and Takayanagi H 2002 Phys. Rev. Lett. **89** 046801
  - 17 Sun Qing-feng and Xie X C 2005 Phys. Rev. B **71** 155321  
Sun Qing-feng, Wang Jian and Guo Hong 165310 Phys. Rev. B **71** 165310
  - 18 Stevens M J, Smirl A L, Bhat R D R, Najmaie A, Sipe J E and van Driel H M 2003 Phys. Rev. Lett. **90** 136603
  - 19 Ganichev S D, Schneider P, Bel'kov V V, Ivchenko E L, Tarasenko S A, Wegscheider W, Weiss D, Schuh D, Murdin B N, Phillips P J, Pidgeon C R, Clarke D G, Merrich M, Murzyn P, Bregulin E V and Prettl W 2003 Phys. Rev. B **68** 081302(R)
  - 20 Najmaie A, Smirl A L and Sipe J E 2005 Phys. Rev. B **71**

- 075306  
Sherman E Y, Najmaie A and Sipe J E 2005 Appl. Phys. Lett. **86** 122103  
Cheng J L and Wu M W 2005 Appl. Phys. Lett. **86** 32107
- <sup>21</sup> Fedorov A, Pershin Y V and Piermarocchi C 2005 Phys. Rev. B **72** 245327  
Pershin Y V and Piermarocchi C 2005 Appl. Phys. Lett. **86** 212107
- <sup>22</sup> Niu C and Lin D L 1997 Phys. Rev. B **56** R12752  
Niu C and Lin D L 2000 Phys. Rev. B **62** 4578
- <sup>23</sup> Zhou Guanghui, Yang Mou, Xiao Xianbo and Li Yuan 2003 Phys. Rev. B **68** 155309
- <sup>24</sup> Meir Y and Wingreen N S 1992 Phys. Rev. Lett **68** 2512  
Jauho A P, Wingreen N S and Meir Y 1994 Phys. Rev. B **50** 5528
- <sup>25</sup> Lee M and Bruder C 2005 Phys. Rev. B **72** 045353  
Lee M and Choi M S 2005 Phys. Rev. B **71** 153306
- <sup>26</sup> Yang M and Li S S 2004 Phys. Rev. B **70** 045318
- <sup>27</sup> Chen G H and Raikh M E 1999 Phys. Rev. B **60** 4826